

# A Mathematical Model for Simulation of Vasoplegic Shock and Vasopressor Therapy

Yi-Ming Kao, Catherine M. Sampson, Syed A. Shah, John R. Salsbury, Ali Tivay, Ramin Bighamian  
Christopher G. Scully, Michael Kinsky, George C. Kramer, and Jin-Oh Hahn, *Senior Member, IEEE*

**Abstract— Objective:** To develop a high-fidelity mathematical model intended to replicate the cardiovascular (CV) responses of a critically ill patient to vasoplegic shock-induced hypotension and vasopressor therapy. **Methods:** The mathematical model consists of a lumped-parameter CV physiology model with baroreflex modulation feedback and a phenomenological dynamic dose-response model of a vasopressor. The adequacy of the proposed mathematical model was investigated using an experimental dataset acquired from 10 pigs receiving phenylephrine (PHP) therapy after vasoplegic shock induced via sodium nitroprusside (SNP). **Results:** Upon calibration, the mathematical model could (i) faithfully replicate the effects of PHP on dynamic changes in blood pressure (BP), cardiac output (CO), and systemic vascular resistance (SVR) (root-mean-squared errors between measured and calibrated mathematical responses: mean arterial BP 2.5+/-1.0 mmHg, CO 0.2+/-0.1 lpm, SVR 2.4+/-1.5 mmHg/lpm; r value: mean arterial BP 0.96+/-0.01, CO 0.65+/-0.45, TPR 0.92+/-0.10) and (ii) predict physiologically plausible behaviors of unmeasured internal CV variables as well as secondary baroreflex modulation effects. **Conclusion:** This mathematical model is perhaps the first of its kind that can comprehensively replicate both primary (i.e., direct) and secondary (i.e., baroreflex modulation) effects of a vasopressor drug on an array of CV variables, rendering it ideally suited to pre-clinical virtual evaluation of the safety and efficacy of closed-loop control algorithms for autonomous vasopressor administration once it is extensively validated. **Significance:** This mathematical model architecture incorporating both direct and baroreflex modulation effects may generalize to serve as part of an effective platform for high-fidelity in silico simulation of CV responses to vasopressors during vasoplegic shock.

**Index Terms—**Vasopressor, Vasoplegia, Phenylephrine, Digital twin, Autonomous critical care, Physiological closed-loop control

## I. INTRODUCTION

VASOPLEGIA is a state of uncontrolled vasodilation that can occur after sepsis, cardiopulmonary bypass and other surgical procedures, ischemia reperfusion, hemorrhage, burns, etc. [1], [2]. Vasopressor administration for maintaining blood pressure (BP) at a target level has long been the widely used approach to vasoplegia treatment in clinical practice [3]. It has

been widely observed that critically ill patients are susceptible to frequent episodes of hypotension, probably due to challenges associated with clinicians' bandwidth to continuously monitor a patient's hemodynamics, control an infusion pump, and maintain the patient's BP at a target level [4], [5]. Hence, there has been an increasing interest in developing computerized systems to automatically titrate vasopressors to maintain a patient's BP [6], [7].

Understanding the performance of computerized automated therapeutic systems requires extensive performance evaluation. Credible evaluation must cover a wide range of physiological responses and disturbance scenarios they may be presented with in clinical environments, in terms of not only the therapeutic endpoints (e.g., BP in the case of vasopressors) but also the overall physiological state (e.g., key cardiovascular (CV) variables such as cardiac output (CO) and systemic vascular resistance (SVR)). Demonstrating such performance under diverse conditions with in vivo animal and human subject studies alone can be challenging due to the excessive amount of requisite time and cost. Hence, computational modeling and simulation technology can potentially reduce the time and cost burdens of in vivo studies as well as to enable extensive stress testing of computerized automated therapeutic systems in the extremes of physiological states [8]–[11].

A therapeutic drug administered to a patient typically elicits multifaceted physiological responses in the patient, which are aggregated to elicit the change in the treatment endpoint. In the case of vasopressor administration, although the treatment endpoint is usually an increase in BP, different vasopressors increase BP in different ways (i.e., by cardiac changes, vascular changes, or both). Hence, a mathematical model suited to the in silico evaluation of computerized vasopressor administration systems must be able to simulate not only the BP response in a patient itself but also various physiological mechanisms (i.e., actuations) responsible for the BP response. Specifically,

This work was supported by the Congressionally Directed Medical Research Programs (Grant W81XWH-19-1-0322) and the U.S. National Science Foundation CAREER Award (Grant CNS-1748762). The mention of commercial products, their sources, or their use in connection with material reported herein is not to be construed as either an actual or implied endorsement of such products by the Department of Health and Human Services.

Y.M. Kao, A.Tivay, and J.O. Hahn are with the Department of Mechanical Engineering, University of Maryland, College Park, MD 20742, USA

(correspondence e-mail: [jhahn12@umd.edu](mailto:jhahn12@umd.edu)). C.M. Sampson, S.A. Shah, J.R. Salsbury, M. Kinsky, and G.C. Kramer are with the Department of Anesthesiology, University of Texas Medical Branch, Galveston, TX 77555, USA. R. Bighamian and C.G. Scully are with the Office of Science and Engineering Laboratories, Center for Devices and Radiological Health, U.S. Food and Drug Administration, Silver Spring, MD 20903, USA.

observed BP response to a vasopressor consists of CV variables (e.g., CO, SVR, and venous blood volume (BV)) subject to primary drug effects and secondary baroreflex modulation effects (i.e., autonomic-cardiac feedback) [12]. In this regard, prior work has not properly distinguished the drug effects and the baroreflex modulation effects in simulating the physiological response to vasopressors. Rather, experimentally observed effects were regarded as vasopressor effects with no explicit account for baroreflex modulation effects. In a prior work on epinephrine (EPI) [13], a set of EPI-specific CV parameters (including ventricular end-systolic elastances and arterial and pulmonary elastances) were estimated at multiple levels of EPI infusion rates. However, there was no account for pharmacokinetics-pharmacodynamics (PKPD) and autonomic-cardiac regulatory feedback. Hence, those EPI-specific parameters thus estimated represented the combined effects of both EPI and autonomic-cardiac regulatory compensation in the steady state. In addition, dynamic changes in the EPI-specific parameters and the resulting change in BP cannot be simulated. In some prior work [14], [15], empiric PKPD models were used to simulate the effects of vasopressors (including phenylephrine (PHP), dopamine (DOP), and dobutamine (DOB)) on BP, but again with no account for baroreflex feedback. Hence, the BP response represents the combined effects of vasopressor and autonomic-cardiac regulatory compensation. In addition, these mathematical models cannot simulate vasopressor-induced changes in CV variables other than BP (such as CO, SVR, and venous BV), which may be important in assessing the safety profile of the computerized vasopressor administration systems. In a prior work on norepinephrine (NEP) [7], the effects of NEP on arterial resistance and venous capacitance were modeled by a Frank-Starling-baroreceptor CV system model and a re-circulatory PKPD model [16]. However, the baroreflex modulation effects in the Frank-Starling-baroreceptor CV system model were incomplete: it included heart rate (HR) compensation but missed SVR and venous BV compensation (which is important in that NEP alters SVR as well as stressed and unstressed venous BV [17], and may also elicit baroreflex modulation effects on these variables). In another prior work on NEP, the effects of NEP on BP through heart rate and SVR was modeled as a black-box model [18]. The structure of the mathematical model correctly captured the interaction of direct NEP effects and secondary baroreflex effects. However, the mathematical model adopted linear transfer functions which may have limitations in replicating NEP PKPD across a wide range. In that vasopressors affect only a subset of CV variables while the remaining CV variables are all affected by baroreflex modulation, the ability to separately replicate the effects of vasopressors and baroreflex modulation may be an important attribute of a mathematical model intended for use in the *in silico* evaluation of computerized vasopressor administration systems. Hence, there are research gaps and rooms for potential improvement in the development of mathematical models that can simulate a comprehensive set of physiological responses to vasopressors, which are critical to assessing the holistic safety and efficacy profile of emerging computerized vasopressor administration

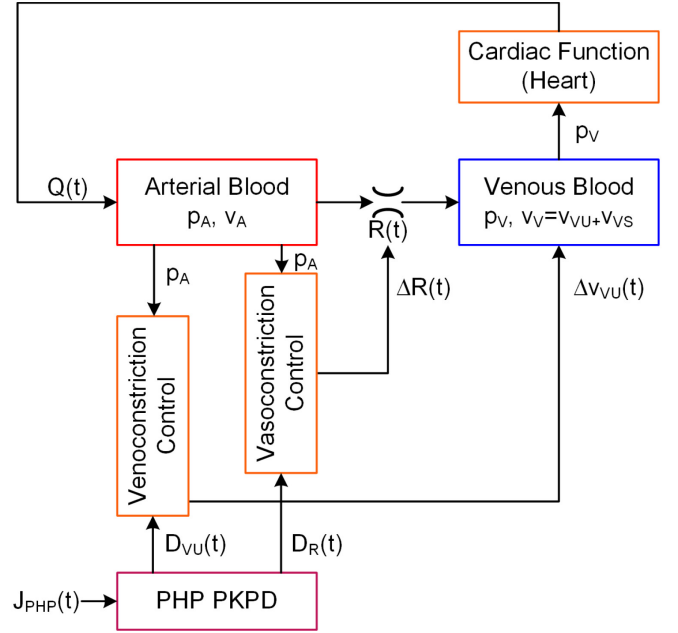


Fig. 1. Mathematical model capable of simulating direct drug-induced and secondary baroreflex modulation effects of phenylephrine (PHP) administration on cardiovascular variables.  $v_A, v_V$ : arterial and venous blood volumes.  $v_{VU}, v_{VS}$ : unstressed and stressed venous blood volumes.  $p_A, p_V$ : arterial and venous blood pressures.  $Q$ : cardiac output.  $R$ : systemic vascular resistance.  $\Delta R, \Delta v_{VU}$ : deviations in  $R$  and  $v_{VS}$  from initial steady-state values.  $J_{PHP}$ : PHP infusion rate.  $D_R, D_{VU}$ : PHP-induced changes in systemic vascular resistance and unstressed venous blood volume.

systems.

This paper presents a high-fidelity mathematical model intended to replicate the CV responses of a critically ill patient to vasoplegic shock-induced hypotension and PHP-based therapy. The mathematical model is perhaps the first of its kind that can comprehensively replicate both direct and baroreflex modulation effects of PHP on an array of CV variables, rendering it ideally suited to pre-clinical virtual evaluation of the safety and efficacy profile of computerized vasopressor administration systems once it is extensively validated. In addition, the modeling methodology can be readily generalized to build mathematical models that can simulate the drug-induced and compensatory responses to various vasopressors.

## II. METHODS

### A. Mathematical Model

The mathematical model was developed by improving a lumped-parameter CV physiology model with baroreflex modulation feedback [19], [20] and integrating into it a phenomenological dynamic vasopressor dose-response model developed in our prior work [21]. In this way, the mathematical model is equipped with all the physiological mechanisms required to simulate both direct and secondary effects of PHP administration (Fig. 1).

CV hemodynamics is given by the conservation of BV:

$$\dot{v}_A(t) = Q(t) - \frac{p_A(t) - p_V(t)}{R(t)}, \quad \dot{v}_V(t) = \frac{p_A(t) - p_V(t)}{R(t)} - Q(t) \quad (1)$$

where  $v_A$  and  $v_V$  are arterial and venous blood volume (BV),  $p_A$  and  $p_V$  are arterial and venous BP,  $Q$  is CO, and  $R$  is SVR. BP

and BV are related by  $\Delta p_A = K_A \Delta v_A$  and  $\Delta p_V = K_V (\Delta v_V - \Delta v_{VU})$ , where  $K_A$  and  $K_V$  are arterial and venous elastances,  $v_{VU}$  is unstressed venous BV, and  $\Delta p_A = p_A - p_{A0}$ ,  $\Delta p_V = p_V - p_{V0}$ ,  $\Delta v_A = v_A - v_{A0}$ ,  $\Delta v_V = v_V - v_{V0}$ , and  $\Delta v_{VU} = v_{VU} - v_{VU0}$  are the deviations of the respective variables from initial steady-state values.

Cardiac function is given by a phenomenological model that replicates the regulation of CO against perturbations in preload (i.e.,  $p_V$ ) [19]:

$$\dot{x}_Q(t) = -p_Q x_Q(t) + (z_Q - p_Q) \Delta P_V(t) \quad (2a)$$

$$\Delta Q(t) = K_Q [x_Q(t) + \Delta P_V(t)] \quad (2b)$$

where  $x_Q$  is an internal state describing the CO dynamics, and  $K_Q$ ,  $p_Q$ , and  $z_Q$  are the parameters characterizing the cardiac function. Note that (2) dictates that  $\Delta Q$  caused by  $\Delta P_V$  (e.g., due to PHP) reduces to  $K_Q \frac{z_Q}{p_Q} \Delta P_V$  as  $t \rightarrow \infty$ , meaning that it can replicate the asymptotic recovery of CO against perturbations in  $\Delta P_V$  if  $K_Q$ ,  $p_Q$ , and  $z_Q$  are properly chosen so that  $K_Q \frac{z_Q}{p_Q} \ll 1$ .

The changes in SVR and unstressed venous BV due to PHP administration and baroreflex modulation are likewise expressed by phenomenological models [19], [20]:

$$\begin{aligned} \dot{x}_R(t) &= -\tau_R x_R(t) - K_R \Delta P_A(t) \\ \Delta R(t) &= x_R(t) + D_R(t) \end{aligned} \quad (3a)$$

$$\begin{aligned} \dot{x}_{VU}(t) &= -\tau_{VU} x_{VU}(t) - K_{VU} \Delta P_A(t) \\ \Delta v_{VU}(t) &= x_{VU}(t) + D_{VU}(t) \end{aligned} \quad (3b)$$

where  $x_R(t)$  and  $x_{VU}(t)$  are internal states describing the SVR and unstressed venous BV,  $K_R$  and  $\tau_R$  are the sensitivity and time constant associated with the baroreflex-based SVR control, and  $K_{VU}$  and  $\tau_{VU}$  likewise are the sensitivity and time constant associated with the baroreflex-based venoconstriction control. The terms  $D_R(t)$  and  $D_{VU}(t)$  are the PHP-induced changes in SVR and unstressed venous BV. From (2)-(3), CO, SVR, and unstressed venous BV are given by  $Q = \Delta Q + Q_0$ ,  $R = \Delta R + R_0$ , and  $v_{VU} = \Delta v_{VU} + v_{VU0}$ , where  $Q_0$ ,  $R_0$ , and  $v_{VU0}$  are initial steady-state values to be estimated. The stressed venous BV is given by  $v_{VS} = v_V - v_{VU}$ .

The pharmacokinetics (PK) and pharmacodynamics (PD) of PHP is given by a dose-response model relating the infusion rate of PHP to its vasoconstriction and venoconstriction effects. The PK of PHP is expressed by a first-order dynamics [21]:

$$\dot{I}_{PHP}(t) = -k_{PHP} I_{PHP}(t) + k_{PHP} J_{PHP}(t) \quad (4)$$

where  $J_{PHP}$  is the intravenous PHP infusion rate and  $I_{PHP}$  is the hypothetical PHP infusion rate at the site of drug action (i.e., arterial and venous blood vessels), while  $\frac{1}{k_{PHP}}$  is the PK time constant. The PD of PHP is given by nonlinear functions relating  $I_{PHP}$  to the increase in SVR and the decrease in unstressed venous BV [21]:

$$D_R(t) = R_0 k_\sigma \ln \frac{x_R(t)}{2 - x_R(t)}, \quad x_R(t) = 1 - \frac{I_{PHP}^{\lambda_R}(t)}{I_{\sigma,R}^{\lambda_R} + I_{PHP}^{\lambda_R}(t)} \quad (5a)$$

$$D_{VU}(t) = \eta_{VU} v_0 \frac{I_{PHP}^{\lambda_{VU}}(t)}{I_{\sigma,VU}^{\lambda_{VU}} + I_{PHP}^{\lambda_{VU}}(t)} \quad (5b)$$

where  $R_0$  and  $v_0 = v_{A0} + v_{V0}$  denote initial steady-state values of SVR and BV, a user-specifiable parameter  $0 < \sigma < 100$  denotes a certain percentage of the maximum vasoconstriction

effect of PHP,  $k_\sigma = -0.01 \frac{\sigma}{\ln 3}$  is a constant,  $I_{\sigma,R}$  and  $I_{\sigma,VU}$  are the hypothetical PHP infusion rates at the site of action corresponding to  $\sigma\%$  of maximum vasoconstriction and venoconstriction effects,  $\lambda_R$  and  $\lambda_{VU}$  are cooperativity constants defining the nonlinearity of dose-response relationships, and  $\eta_{VU}$  denotes the fraction of BV that can be involved in venoconstriction. The value of  $\eta_{VU}$  was set to 0.21 based on the literature [22], [23]. It is noted that  $x_R(t)$  decreases from unity to zero as  $I_{PHP}$  increases, which in turn leads to  $\frac{x_R}{2 - x_R} \rightarrow 0$  as  $I_{PHP} \rightarrow \infty$ , resulting in  $D_R \rightarrow \infty$ , i.e.,  $D_R$  increases as  $I_{PHP}$  increases.

For an individual subject  $i$ , the mathematical model is characterized by the vector of parameters  $\theta_i$  given by:

$$\theta_i = \{K_A, K_V, K_Q, p_Q, z_Q, K_R, \tau_R, K_{VU}, \tau_{VU}, k_{PHP}, I_{\sigma,R}, \lambda_R, I_{\sigma,VU}, \lambda_{VU}, p_{A0}, p_{V0}, v_0, v_{VU0}, Q_0\} \quad (6)$$

Note that (6) includes 5 initial condition parameters for arterial BP ( $p_{A0}$ ), CVP ( $p_{V0}$ ), BV ( $v_0$ ), unstressed venous BV ( $v_{VU0}$ ), and CO ( $Q_0$ ).

## B. Experimental Dataset

To investigate the preliminary adequacy of the mathematical model in replicating CV responses to PHP administration, we performed a calibration exercise using an in vivo dataset consisting of data collected from 10 anesthetized pigs. The experiments were conducted at the University of Texas Medical Branch under the approval of its Institutional Animal Care and Use Committee (IACUC; approval number: 1907063).

In each animal, anesthesia was induced with ketamine and telazol and then maintained with propofol until the study ended. Surgical procedures were performed to place a femoral artery catheter for arterial BP monitoring as well as a femoral venous catheter for the administration of PHP and a second femoral venous catheter for the administration of sodium nitroprusside (SNP). In addition, a catheter was placed in the jugular vein, through which a Swan-Ganz catheter was inserted for monitoring of cardiac functions (including CO and central venous pressure (CVP)).

Each animal was instrumented for its baseline state for >30 min before any interventions were given. Then, the animal received 10-min infusions of PHP concentrated at 40mcg/ml at multiple rates ranging 10-120 ml/hr. In a subset of animals (N=4), SNP was infused to induce vasoplegic shock [24]. SNP was given at a constant infusion rate tailored in each animal to achieve mean arterial BP of 30-60 mmHg. During the course of the experiment, arterial BP and CVP were measured at a sampling rate of 1 kHz, while CO was measured every 10 min.

From the collected data, beat-by-beat mean arterial BP and CVP were computed as the intra-beat average of arterial BP and CVP signals. At the times CO was measured, SVR was computed by subtracting CVP from mean arterial BP and then dividing the difference by the measured CO. Finally, the beat-by-beat mean arterial BP and the intermittently measured CO and SVR were subsequently used to assess the adequacy of the mathematical model.

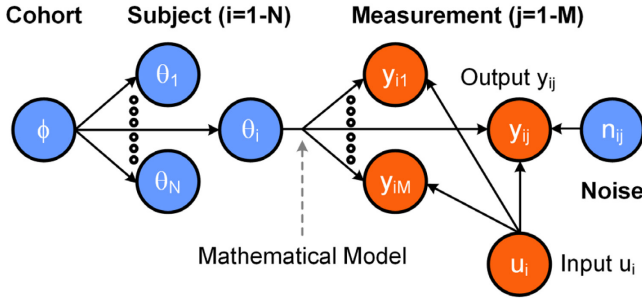


Fig. 2. A probabilistic graphical model (PGM) that structures the hierarchical relationship between a cohort and subjects therein.

### C. System Identification via Collective Variational Inference

To execute the calibration exercise, we employed a novel computational algorithm developed in our prior work called the collective variational inference (C-VI) method (code repository: <https://github.com/alitvay/collective-variational-inference.git>) [19]. For a mathematical model, the C-VI method analyzes a dataset including data collected from a cohort of subjects to calibrate the mathematical model to all the subjects in the cohort and derive subject-specific parameters, as well as to infer cohort-level parameters representative of (i.e., capturing the commonalities of) all the subjects belonging to the cohort. It fulfills these tasks by structuring the hierarchical relationship between a cohort and subjects therein in the form of the probabilistic graphical model (PGM) in Fig. 2. The PGM embodies the reliance of the inputs ( $u_i$ 's) given to and outputs ( $y_{ij}$ 's) created by the mathematical model on the latent parameters that characterize the cohort-level mathematical model parameters ( $\phi$ ), subject-specific mathematical model parameters ( $\theta_i$ 's), and measurement noise ( $n_{ij}$ 's). Here,  $\phi$  denotes the beliefs on the cohort-level mathematical model parameters, while  $\theta_i$  denotes the beliefs on the mathematical model parameters associated with subject  $i$  (both in the form of diagonal Gaussian densities).  $y_{ij}$  is the output  $j$  in subject  $i$ , which can be computed by giving the inputs  $u_i$  to the mathematical model in II.A parameterized with  $\theta_i$ .  $n_{ij}$  denotes the standard deviation (SD) of the Gaussian noise corrupting  $y_{ij}$ .

The C-VI method estimates the latent parameters in the PGM from the given dataset by inferring the posterior density:

$$p(\phi, \theta, \mathbf{n} | \mathbf{u}, \mathbf{y}) = \frac{p(\phi, \theta, \mathbf{n}, \mathbf{u}, \mathbf{y})}{p(\mathbf{u}, \mathbf{y})} \quad (7)$$

where  $p(\phi, \theta, \mathbf{n}, \mathbf{u}, \mathbf{y}) = p(\phi)p(\theta|\phi)p(\mathbf{y}|\theta, \mathbf{n}, \mathbf{u})p(\mathbf{n})p(\mathbf{u})$  and  $\theta$ ,  $\mathbf{n}$ ,  $\mathbf{u}$ , and  $\mathbf{y}$  denote the collections of all the latent parameters  $\theta_i$ 's and  $n_{ij}$ 's as well as the data  $u_i$ 's and  $y_{ij}$ 's. Noting that inferring the posterior density in (7) is not usually tractable, the C-VI method exploits modern variational inference techniques [25], [26] to define an approximate posterior density  $q(\phi, \theta, \mathbf{n} | \mathbf{v})$  and infer it by minimizing the K-L divergence  $D_{KL}(\mathbf{v})$  between  $p$  in (7) and  $q$  with respect to the variational parameters  $\mathbf{v}$ , which in the case of this paper defines mean and SD of the elements in  $q$  expressed by a family of diagonal Gaussian densities:

$$D_{KL}(\mathbf{v}) = \mathbb{E}_q[\log q(\phi, \theta, \mathbf{n} | \mathbf{v}) - \log p(\phi, \theta, \mathbf{n} | \mathbf{u}, \mathbf{y})] \quad (8)$$

The C-VI method estimates  $\mathbf{v}$  by maximizing the evidence lower bound (ELBO) in (9), obtained from (7)-(8), based on stochastic optimization algorithms [27], [28]:

$$\begin{aligned} L(\mathbf{v}) &= \log p(\mathbf{y}) - D_{KL}(\mathbf{v}) \\ &= \mathbb{E}_q[\log p(\mathbf{y} | \theta, \mathbf{n}, \mathbf{u}) + \log p(\theta | \phi) + \log p(\mathbf{n}) + \log p(\phi) - \log q(\phi, \theta, \mathbf{n} | \mathbf{v})] \end{aligned} \quad (9)$$

Finally, the mathematical model parameters calibrated to each subject (i.e.,  $\theta_i$  in (6)) as well as the cohort-level mathematical model parameters ( $\phi$  in Fig. 2) can be obtained from  $\mathbf{v}$ . Full details of the C-VI method are described in [19].

### D. Mathematical Model Evaluation

We calibrated the mathematical model in II.A by fitting it to the dataset in II.B. With the goal of establishing the initial adequacy of the mathematical model as a basis to replicate CV response to PHP, we used the entire dataset, i.e., the entire time period of all the animals pertaining to PHP administration. Leveraging the C-VI method in II.C, we derived both subject-specific and cohort-level probability density distributions of all the mathematical model parameters in (6) by maximizing the ELBO in (9) in conjunction with the mathematical model and the experimental data. Then, the preliminary adequacy of the mathematical model was evaluated in several aspects. First, its ability to replicate experimentally observed CV responses was assessed via calibration accuracy in terms of the root-mean-squared errors (RMSEs) and  $r$  values associated with mean arterial BP, CO, and SVR. Second, its physiological plausibility was assessed by examining the legitimacy of the simulated internal (i.e., unmeasured) CV variables (including arterial and venous BVs). Third, its practical identifiability characteristics was assessed by comparing subject-specific and cohort-level distributions of the mathematical model parameters derived from the C-VI method. Fourth, we analyzed the effect of sample size and omitting subcomponent models (including PHP-induced vasoconstriction and venoconstriction, by setting  $D_R(t) = D_{VU}(t) = 0$  in (3), as well as baroreflex-based modulation of vasoconstriction and venoconstriction, by setting  $K_R = K_{VU} = 0$ ) in the mathematical model on the C-VI inference outcomes.

## III. RESULTS

Table 1 shows the RMSEs and  $r$  values associated with subject-specific calibration, i.e., fitting the mathematical model to the data pertaining to individual animals. Fig. 3 shows a representative example of mathematical model simulations in the (a) absence and (b) presence of SNP-induced vasoplegic shock in an animal, including (i) measured mean arterial BP, CO, and SVR versus the same variables predicted by the calibrated mathematical model (which are of importance due to PHP's vasoconstriction effects) as well as (ii) internal (i.e., unmeasured) CV variables of arterial BV and unstressed venous BV predicted by the calibrated mathematical model (which are of importance due to PHP's venoconstriction effects). In Fig. 3, "net effect" means "PHP effect" minus the baroreflex modulation effect. Fig. 4 compares (a) direct PHP responses and (b) net responses in SVR and unstressed venous BV as well as (c) cardiac sensitivity in the absence vs presence of SNP-

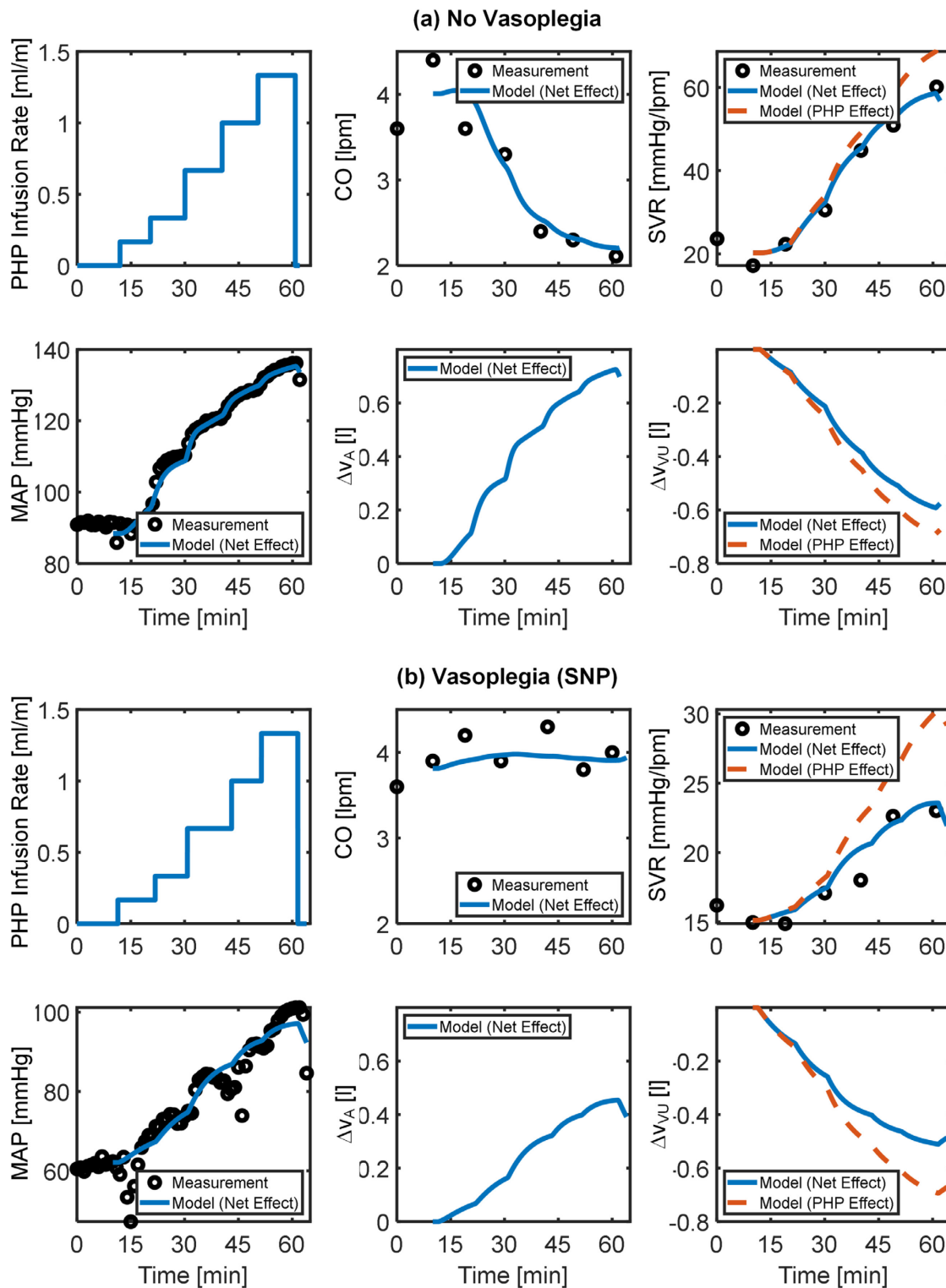


Fig. 3. Representative example of measured versus subject-specific fitted mean arterial BP, CO, and SVR responses and internal (i.e., unmeasured) CV variables predicted by the mathematical model in an animal. (a) No vasoplegia (SNP). (b) Vasoplegia (SNP).  $\Delta v_A$ : change in arterial blood volume.  $\Delta v_{VU}$ : change in unstressed venous blood volume.

induced vasoplegia. Fig. 5 shows the probability density distributions of the mathematical model parameters, except the initial conditions  $p_{A0}$ ,  $p_{V0}$ ,  $v_{VU0}$ , and  $Q_0$  (whose distributions were trivially consistent with the experimental data as well as anticipated trends), in the (a) absence and (b) presence of SNP-induced vasoplegic shock. The parametric distributions

pertaining to the absence of vasoplegic shock (“No SNP” in Fig. 5) were derived from the 11 data corresponding to the 10 pigs which did not receive SNP (one animal received 2 PHP infusion interventions), while those pertaining to the presence of vasoplegic shock (“SNP” in Fig. 5) were derived from the 4 data corresponding to the 4 pigs which received SNP. Fig. 6

TABLE I

Root-mean-squared errors (RMSEs) and  $r$  values associated with subject-specific fitting. RMSEs and  $r$  values were computed in each animal using all the measurements, and then were summarized as mean $\pm$ SD.

		No SNP	SNP	All
MAP	RMSE [mmHg]	2.1 $\pm$ 0.6	3.0 $\pm$ 1.0	2.5 $\pm$ 1.0
	$r$	0.96 $\pm$ 0.01	0.96 $\pm$ 0.01	0.96 $\pm$ 0.01
CO	RMSE [lpm]	0.2 $\pm$ 0.1	0.1 $\pm$ 0.1	0.2 $\pm$ 0.1
	$r$	0.82 $\pm$ 0.21	0.31 $\pm$ 0.54	0.65 $\pm$ 0.45
SVR	RMSE [mmHg/lpm]	2.7 $\pm$ 1.3	1.6 $\pm$ 1.1	2.4 $\pm$ 1.5
	$r$	0.94 $\pm$ 0.06	0.87 $\pm$ 0.15	0.92 $\pm$ 0.10

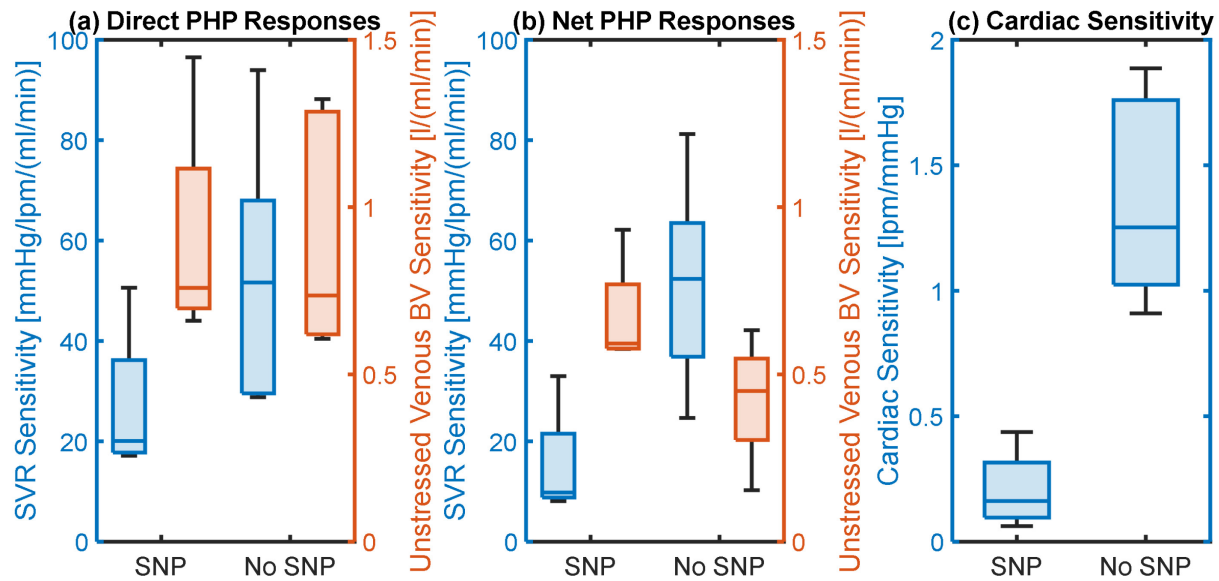


Fig. 4. Comparison of (a) direct PHP responses and (b) net responses in SVR and unstressed venous BV as well as (c) cardiac sensitivity in the absence vs presence of SNP-induced vasoplegia. The responses and sensitivity were calculated by dividing the response corresponding to the maximum dose by the maximum dose itself (which is an indicative of the slope of the dose-response relationship).

shows the subject-specific and cohort-level probability density distributions of the mathematical model parameters. Each plot shows the cohort-level probabilistic distribution of a parameter (“Cohort-Level” in Fig. 6) and 15 subject-specific probabilistic distribution of the same parameter associated with the 10 animals (“Subject-Specific” in Fig. 6). Table II compares the RMSEs associated with subject-specific calibration of the mathematical model when subcomponent models were omitted.

#### IV. DISCUSSION

There are various CV variable responses involved in the mechanisms of action of the vasopressor, e.g., CO, SVR, and unstressed venous BV, which are affected by both the direct drug effects and the secondary baroreflex modulation effects. A mathematical model suited to the *in silico* evaluation of computerized vasopressor systems must ideally be able to simulate all these CV variable responses in detail. This paper presents a mathematical model capable of simulating the effects of PHP on mean arterial BP as well as the physiological mechanisms involved in PHP-induced changes in mean arterial BP (i.e., vasoconstriction and venoconstriction).

Once fitted to each animal, the mathematical model could replicate the experimentally measured CV variable responses of BP, CO, and SVR to PHP administration at a wide range of dose

levels (Table 1, Fig. 3). The goodness of fit associated with BP, CO, and SVR appeared to be adequate consistently across all the animals (maximum BP<5.3 mmHg, CO<0.6 lpm, SVR<5.4mmHg/lpm). Remarkably, the mathematical model could replicate CV variable responses both in the absence (Fig. 3(a)) and presence (Fig. 3(b)) of SNP-induced vasoplegia. In addition to the experimentally measured CV variables, the mathematical model predicted physiologically plausible responses in the internal CV variables of arterial BV and venous BV (e.g., relaxed baroreflex modulation effects to hypotension (i.e., vasoconstriction and venoconstriction) in response to PHP administration [29]). All in all, the results suggest that the mathematical model may be able to simulate CV variable responses to PHP under a broad range of vasoplegic shock severity.

Deeper scrutiny of the mathematical model simulations provided additional insights on the impact of vasoplegic shock on the PHP-induced vasoconstriction and venoconstriction effects. For this analysis, we used the data from the 4 pigs containing PHP responses both with and without SNP-induced vasoplegia. Fig. 3 reveals that the resultant change in mean arterial BP in response to PHP was comparable in the absence versus presence of SNP-induced vasoplegia. However, the mechanism underlying the change in mean arterial BP was quite

TABLE II

Root-mean-squared errors (RMSEs) associated with subject-specific fitting of the mathematical model when subcomponent models were omitted. RMSEs were computed in each animal using all the measurements, and then were summarized as mean $\pm$ SD. \*:  $p < 0.05$ .

	MAP RMSE [mmHg]	CO RMSE [lpm]	SVR RMSE [mmHg/lpm]
Mathematical Model w/ No Omission	2.5 $\pm$ 1.0	0.2 $\pm$ 0.1*	2.4 $\pm$ 1.5*
No PHP Effect on SVR	2.7 $\pm$ 1.5	1.0 $\pm$ 0.4*	11 $\pm$ 4.6*
No PHP Effect on Unstressed Venous BV	2.9 $\pm$ 1.2	0.3 $\pm$ 0.2*	3.2 $\pm$ 1.9*
No SVR Baroreflex Effect	2.5 $\pm$ 1.0	0.3 $\pm$ 0.3*	2.9 $\pm$ 1.8*
No Unstressed Venous BV Baroreflex Effect	2.5 $\pm$ 1.1	0.2 $\pm$ 0.2*	2.8 $\pm$ 1.9*

distinct. First, SNP-induced vasoplegia substantially decreased the direct vasoconstriction efficacy of PHP (i.e., in increasing SVR; compare the orange SVR responses in Fig. 3(a) vs Fig. 3(b)) as well as the resultant (i.e., combined PHP and baroreflex modulation) vasoconstriction response (compare the blue SVR responses in Fig. 3(a) vs Fig. 3(b)). This observation appears to be consistent with the existing knowledge related to vascular hypo-reactivity to vasopressors in vasoplegic shock [2]. Second, SNP-induced vasoplegia did not appear to alter the direct venoconstriction efficacy of PHP (i.e., in decreasing unstressed venous BV; compare the orange unstressed venous BV responses in Fig. 3(a) vs Fig. 3(b)), whereas it substantially decreased the resultant venoconstriction response (compare the blue unstressed venous BV responses in Fig. 3(a) vs Fig. 3(b)). This observation suggests that baroreflex modulation pertaining to unstressed venous BV was weakened due to the SNP-induced vasoplegia (in that venoconstriction response when PHP was administered decreased more in vasoplegic condition than in non-vasoplegic condition). But, it is a speculation that needs to be confirmed). Third, SNP-induced vasoplegia lowered cardiac sensitivity (i.e., contractility and heart rate) to the change in preload (i.e., stressed venous BV; as can be seen in much smaller change in CO in the case of SNP-induced vasoplegia in Fig. 3). The above observations are summarized in Fig. 4 using the data aggregated from the 4 pigs. It is noted that the statistical significance of the observed differences was not established due to the small sample size ( $N=4$ ).

The above observations could be ascertained in terms of mathematical model parameters (Fig. 5). First, the PHP PD parameters pertaining to vasoconstriction ( $I_{\sigma,R}$ ,  $\lambda_R$ , and  $R_0$ ) collectively changed to desensitize SVR response to PHP under SNP-induced vasoplegia: (i)  $I_{\sigma,TPR}$  increased (Fig. 5), (ii)  $\lambda_R$  decreased (Fig. 5), and (iii)  $R_0$  decreased (not shown). On the other hand, the PHP PK parameter ( $k_{PHP}$ ) did not notably change. Second, the parameters related to CO ( $K_Q$ ,  $p_Q$ , and  $z_Q$ ) collectively changed to desensitize CO response to the change in preload (i.e.,  $\Delta P_V$ ):  $K_Q$  decreased,  $p_Q$  increased, and  $z_Q$  decreased to decrease the effective gain  $K_Q \frac{z_Q}{p_Q}$  of the CO function. It is noted that the parameters related to the baroreflex modulation of unstressed venous BV (specifically, a decrease in  $K_{VU}$  and an increase in  $\tau_{VU}$  in the case of simulated vasoplegia) indicated its modest desensitization due to vasoplegia, but it was not comparable to the decrease in cardiac sensitivity.

Comparison of subject-specific and cohort-level model parameter distributions revealed that most of the parameters in the mathematical model may be practically identifiable with

frequent mean arterial BP measurement in conjunction with relatively sparse CO and SVR measurements. Using the C-VI method, the practical identifiability of an individual parameter can be (at least qualitatively) assessed by comparing its subject-specific versus cohort-level distributions: a parameter can be viewed practically identifiable if its subject-specific probability density distributions have diverse mean values and spreads narrower than the cohort-level spread. Most parameters in the mathematical model exhibited such characteristics (Fig. 6). Exceptions were a small number of parameters pertaining to the dynamics of baroreflex modulation ( $\tau_r$ ,  $\tau_{VU}$ ,  $z_Q$ ): in many subjects, subject-specific probability density distributions show mean values and spreads quite comparable to the cohort-level probability density distributions. These parameters are associated with time constants much less than a minute and thus may not be accurately inferred with CO and SVR measurement intervals of 10 min. These parameters may exert low sensitivity to the measurements and may not be practically identifiable. However, these parameters may potentially be made practically identifiable by invoking more frequent measurements of CO and SVR, e.g., using pulse contour CO monitors [30].

Comparison of cohort-level model parameter distributions with respect to sample size suggested that the model parameter distributions may be adequate. Indeed, the cohort-level model parameter distributions remained highly consistent even when the sample size used in the C-VI was reduced to 12, 9, and 6. It may thus be concluded that the size of the experimental dataset used in this work is adequate.

Examining the impact of omitting subcomponent models on the quality of the resulting subject-specific mathematical model furnished a few interesting insights on the structural adequacy of the proposed mathematical model. First, the quality (in terms of goodness-of-fit) of the mathematical model was in general deteriorated when a subcomponent model was omitted (Table II). Specifically, BP error was preserved, but CO and/or SVR errors were deteriorated. This may be interpreted as follows: the mathematical model fits the dataset to replicate BP (whose measurement is much more frequent than CO and SVR) while compromising its ability to replicate CO and SVR. In any case, the results indicate that the proposed mathematical model may be structurally adequate. Second, omitting the direct PHP effect components yielded more drastic impact on the goodness-of-fit than omitting the baroreflex control components (i.e., compare “No PHP Effect on SVR” versus “No SVR Baroreflex Effect” as well as “No PHP Effect on Unstressed Venous BV” versus “No Unstressed Venous BV Baroreflex Effect” in Table II). This may be interpreted as follows: (i) when the baroreflex control effect is omitted, the mathematical model absorbs the

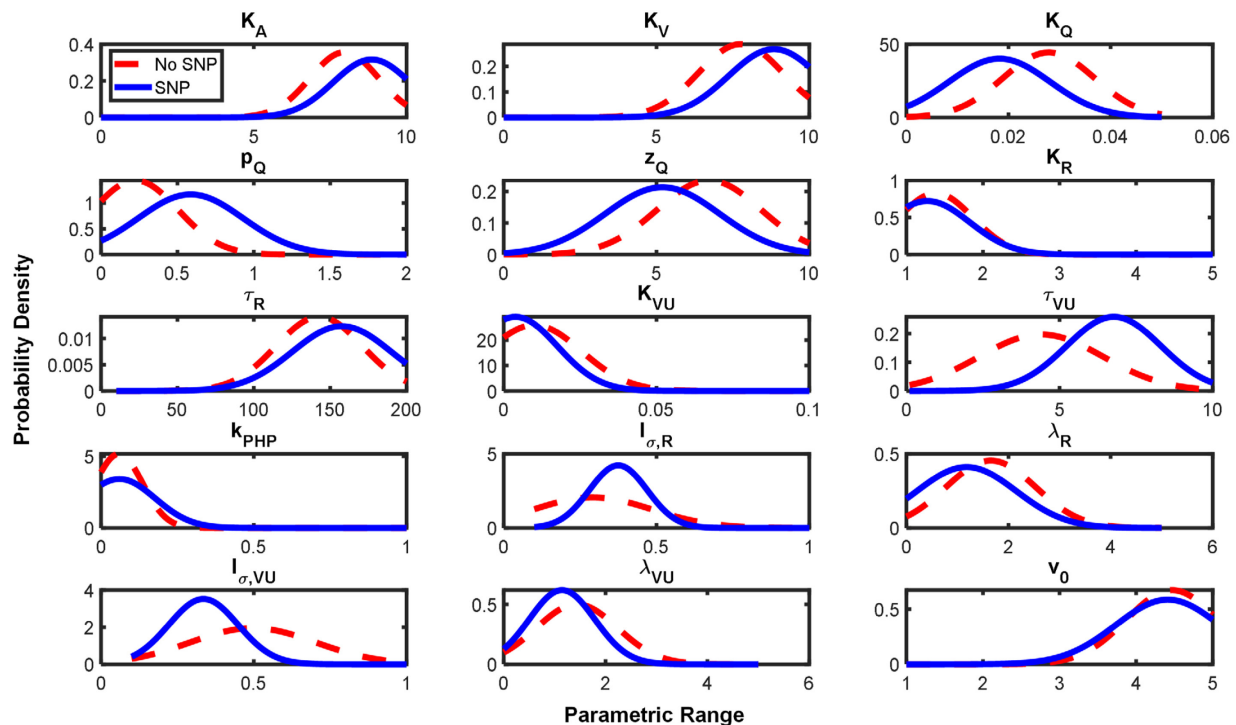


Fig. 5. Cohort-level model parameter distributions associated with no SNP (red dashed) and SNP (blue solid) data.

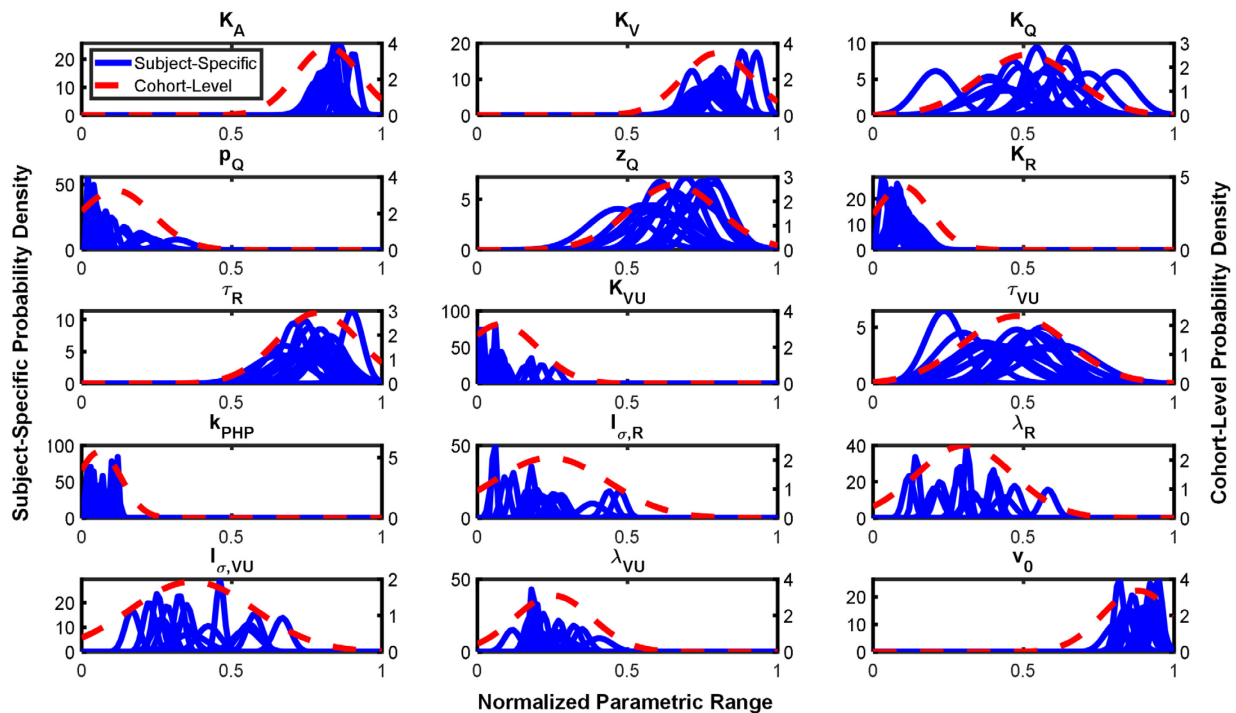


Fig. 6. Subject-specific and cohort-level model parameter distributions (all data). The magnitudes are normalized for ease of comparison. Low-sensitivity parameters ( $\tau_r$ ,  $\tau_{vU}$ , and  $z_Q$ ) tend to exhibit comparable subject-specific and cohort-level distributions.

baroreflex control effect in the PHP dose-response relationship, thereby mitigating the deterioration in the goodness-of-fit; on the contrary, (ii) when the direct PHP effect is omitted, the mathematical model views the PHP-induced changes in BP, CO, and SVR as disturbances caused by unknown sources, thereby making the calibration much more challenging. In any case, although omitting the baroreflex control components does not appear to substantially worsen the goodness-of-fit, it may

still be desirable for a mathematical model to have explicit baroreflex control components in order to replicate various critical care treatment scenarios, since there are many external stimulations other than vasopressors (e.g., hemorrhage) which trigger compensatory vasoconstriction and venoconstriction. Third, omitting the vasoconstriction components yielded more drastic impact than omitting the venoconstriction components (i.e., compare “No PHP Effect on SVR” versus “No PHP Effect

on Unstressed Venous BV” as well as “No SVR Baroreflex Effect” versus “No Unstressed Venous BV Baroreflex Effect” in Table II). This may just be specific to this work in which SVR but not unstressed BV was included in the calibration dataset. Accordingly, it is speculated that including measurements relevant to BV (e.g., hematocrit) in the calibration dataset can increase the relative importance of venoconstriction components.

In summary, the mathematical model presented in this paper was able to faithfully simulate mean arterial BP, CO, and SVR responses to PHP administration as well as predicted physiologically plausible internal variable responses during SNP-induced vasoplegia. The mathematical model also suggests that the potency of PHP in vasoconstriction and the cardiac function may be depressed in the presence of severe vasoplegic shock. Lastly, the mathematical model is to a large extent practically identifiable with frequent mean arterial BP and intermittent CO and SVR measurements.

This study has limitations in the context of independent validation: we demonstrated the ability of the mathematical model subject-specifically calibrated to individual animals to replicate the same animals’ responses. However, the mathematical model was not validated with independent experimental datasets. Being able to demonstrate that the mathematical model can accurately reproduce data not presented in the calibration phase would support its use for in silico testing of computerized vasopressor administration systems [10], [31].

## V. CONCLUSION

This paper presented a mathematical model suited for simulating comprehensive CV responses to PHP administration. By virtue of its ability to simulate both direct PHP-induced and secondary baroreflex modulation responses, the mathematical model may play an important role in pre-clinical safety and performance assessment of next-generation computerized PHP administration systems (and perhaps similar systems for a wide range of vasopressors) in the near term pending extensive independent validation. In the longer term, the mathematical model may be extended to have the capability to simulate more complex polytrauma scenarios, making it even more suited to assess the safety and efficacy of a wide range of computerized trauma resuscitation systems. Such a potential impact of the mathematical model is highly responsive to the emerging interest in medical digital twins and its use in efficient pre-clinical evaluation of physiological closed-loop control systems. Hence, future work directed to the application of the mathematical model to pre-clinical evaluation of automated PHP administration systems as well as the extension of the mathematical model to enable its use for various vasopressors, other intravenous drugs (e.g., sedatives and opioids), and fluids and blood products will further its utility and impact.

## REFERENCES

- [1] S. Lambden, B. C. Creagh-Brown, J. Hunt, C. Summers, and L. G. Forni, “Definitions and Pathophysiology of Vasoplegic Shock,” *Critical Care*, vol. 22, no. 1. BioMed Central Ltd., Jul. 06, 2018. doi: 10.1186/s13054-018-2102-1.
- [2] B. Levy, C. Fritz, E. Tahon, A. Jacquot, T. Auchet, and A. Kimmoun, “Vasoplegia Treatments: The Past, the Present, and the Future,” *Critical Care*, vol. 22, no. 1. BioMed Central Ltd., Feb. 27, 2018. doi: 10.1186/s13054-018-1967-3.
- [3] M. Egi *et al.*, “Selecting a Vasopressor Drug for Vasoplegic Shock After Adult Cardiac Surgery: A Systematic Literature Review,” *Ann Thorac Surg*, vol. 83, no. 2, pp. 715–723, Feb. 2007. doi: 10.1016/j.athoracsur.2006.08.041.
- [4] G. Hawryluk *et al.*, “Mean Arterial Blood Pressure Correlates with Neurological Recovery after Human Spinal Cord Injury: Analysis of High Frequency Physiologic Data,” *J Neurotrauma*, vol. 32, no. 24, pp. 1958–1967, Feb. 2015. doi: 10.1089/neu.2014.3778.
- [5] B. Yapps *et al.*, “Hypotension in ICU Patients Receiving Vasopressor Therapy,” *Sci Rep*, vol. 7, no. 1, p. 8551, 2017. doi: 10.1038/s41598-017-08137-0.
- [6] O. Desebbe *et al.*, “Control of Postoperative Hypotension Using a Closed-Loop System for Norepinephrine Infusion in Patients After Cardiac Surgery: A Randomized Trial,” *Anesth Analg*, vol. 134, no. 5, pp. 964–973, May 2022. doi: 10.1213/ane.0000000000005888.
- [7] J. Rinehart, A. Joosten, M. Ma, M.-D. Calderon, and M. Cannesson, “Closed-Loop Vasopressor Control: In-Silico Study of Robustness against Pharmacodynamic Variability,” *J Clin Monit Comput*, vol. 33, no. 5, pp. 795–802, 2019. doi: <http://dx.doi.org/10.1007/s10877-018-0234-0>.
- [8] M. Viceconti, F. Pappalardo, B. Rodriguez, M. Horner, J. Bischoff, and F. Musuamba Tshinanu, “In Silico Trials: Verification, Validation and Uncertainty Quantification of Predictive Models Used in the Regulatory Evaluation of Biomedical Products,” *Methods*, vol. 185, pp. 120–127, Jan. 2021. doi: 10.1016/j.ymeth.2020.01.011.
- [9] B. Parvinian, C. Scully, H. Wiyor, A. Kumar, and S. Weinger, “Regulatory Considerations for Physiological Closed-Loop Controlled Medical Devices Used for Automated Critical Care: Food and Drug Administration Workshop Discussion Topics,” *Anesth Analg*, vol. 126, no. 6, pp. 1916–1925, 2018.
- [10] B. Parvinian, R. Bighamian, C. G. Scully, J. O. Hahn, and P. Pathmanathan, “Credibility Assessment of a Subject-Specific Mathematical Model of Blood Volume Kinetics for Prediction of Physiological Response to Hemorrhagic Shock and Fluid Resuscitation,” *Front Physiol*, vol. 12, Sep. 2021. doi: 10.3389/fphys.2021.705222.
- [11] F. Pappalardo, G. Russo, F. M. Tshinanu, and M. Viceconti, “In Silico Clinical Trials: Concepts and Early Adoptions,” *Brief Bioinform*, vol. 20, no. April 2018, pp. 1699–1708, 2018. doi: 10.1093/bib/bby043.
- [12] J. Jordan *et al.*, “Baroreflex Buffering and Susceptibility to Vasoactive Drugs,” *Circulation*, vol. 105, no. 12, pp. 1459–1464, 2002. doi: 10.1161/01.CIR.0000012126.56352.FD.
- [13] J. G. Chase *et al.*, “Model-Based Prediction of the Patient-Specific Response to Adrenaline,” *Open Med Inform J*, vol. 4, pp. 149–163, 2010. doi: 10.2174/1874431101004010149.
- [14] T. Wassar *et al.*, “Automatic Control of Arterial Pressure for Hypotensive Patients using Phenylephrine,” *International Journal of Modeling and Simulation*, vol. 34, no. 4, pp. 187–198, 2014. doi: 10.2316/Journal.205.2014.4.205-6087.
- [15] M. Görges, D. R. Westenskow, K. Kück, and J. a. Orr, “A Tool Predicting Future Mean Arterial Blood Pressure Values Improves the Titration of Vasoactive Drugs,” *J Clin Monit Comput*, vol. 24, pp. 223–235, 2010. doi: 10.1007/s10877-010-9238-0.
- [16] R. N. Upton and G. L. Ludbrook, “Pharmacokinetic-Pharmacodynamic Modelling of the Cardiovascular Effects of Drugs - Method Development and Application to Magnesium in Sheep,” *BMC Pharmacol*, vol. 5, p. 5, 2005. doi: 10.1186/1471-2210-5-5.

- [17] P. Foulon and D. de Backer, “The Hemodynamic Effects of Norepinephrine: Far More than an Increase in Blood Pressure!,” *Ann Transl Med*, vol. 6, no. S1, pp. S25–S25, Nov. 2018, doi: 10.21037/atm.2018.09.27.
- [18] L. Wang, S. Ansari, K. R. Ward, K. Najarian, and K. R. Oldham, “Identification of Compensatory Arterial Dynamics in Swine using a Non-Invasive Sensor for Local Vascular Resistance,” in *Proceedings of the ASME 2018 Dynamic Systems and Control Conference*, 2018, pp. DSCC2018-9063. [Online]. Available: <http://asmedigitalcollection.asme.org/DSCC/proceedings-pdf/DSCC2018/51890/V001T14A002/2376644/v001t14a002-dscc2018-9063.pdf>
- [19] A. Tivay, G. C. Kramer, and J.-O. Hahn, “Collective Variational Inference for Personalized and Generative Physiological Modeling: A Case Study on Hemorrhage Resuscitation,” *IEEE Trans Biomed Eng*, vol. 69, no. 2, pp. 666–677, 2022, doi: 10.1109/TBME.2021.3103141.
- [20] W. Yin, A. Tivay, and J.-O. Hahn, “Hemodynamic Monitoring via Model-Based Extended Kalman Filtering: Hemorrhage Resuscitation and Sedation Case Study,” *IEEE Control Syst Lett*, vol. 6, pp. 2455–2460, 2022, doi: 10.1109/LCSYS.2022.3164965.
- [21] J. Zhu, X. Jin, R. Bighamian, C. Kim, S. T. Shipley, and J. Hahn, “Semi-Adaptive Infusion Control of Medications with Excitatory Dose-Dependent Effects,” *IEEE Transactions on Control Systems Technology*, vol. 27, no. 4, pp. 1735–1743, 2019.
- [22] C. C. Y. Pang, “Autonomic Control of the Venous System in Health and Disease: Effects of Drugs,” *Pharmacol Ther*, vol. 90, no. 2–3, pp. 179–230, May 2001, doi: 10.1016/S0163-7258(01)00138-3.
- [23] S. Gelman, D. S. Warner, and M. A. Warner, “Venous Function and Central Venous Pressure,” *Anesthesiology*, vol. 108, no. 4, pp. 735–748, Apr. 2008, doi: 10.1097/ALN.0b013e3181672607.
- [24] A. Joosten *et al.*, “Automated Titration of Vasopressor Infusion Using a Closed-Loop Controller In Vivo Feasibility Study Using a Swine Model,” *Anesthesiology*, vol. 130, no. 3, pp. 394–403, 2019, [Online]. Available: [http://pubs.asahq.org/anesthesiology/article-pdf/130/3/394/386167/20190300\\_0-00013.pdf](http://pubs.asahq.org/anesthesiology/article-pdf/130/3/394/386167/20190300_0-00013.pdf)
- [25] D. M. Blei, A. Kucukelbir, and J. D. McAuliffe, “Variational Inference: A Review for Statisticians,” *J Am Stat Assoc*, vol. 112, no. 518, pp. 859–877, 2017.
- [26] D. P. Kingma and M. Welling, “An Introduction to Variational Autoencoders,” *Foundations and Trends in Machine Learning*, vol. 12, no. 4, pp. 307–392, 2019, doi: 10.1561/22000000056.
- [27] R. Ranganath, S. Gerrish, and D. M. Blei, “Black Box Variational Inference,” *Journal of Machine Learning Research*, vol. 33, pp. 814–822, 2014.
- [28] M. D. Hoffman, D. M. Blei, C. Wang, and J. Paisley, “Stochastic Variational Inference,” *Journal of Machine Learning Research*, vol. 14, pp. 1303–1347, 2013.
- [29] J. Jordan *et al.*, “Baroreflex buffering and susceptibility to vasoactive drugs,” *Circulation*, vol. 105, no. 12, pp. 1459–1464, Mar. 2002, doi: 10.1161/01.CIR.0000012126.56352.FD.
- [30] J. Grensemann, “Cardiac Output Monitoring by Pulse Contour Analysis, the Technical Basics of Less-Invasive Techniques,” *Frontiers in Medicine*, vol. 5, no. MAR. Frontiers Media S.A., Mar. 01, 2018, doi: 10.3389/fmed.2018.00064.
- [31] R. Bighamian, J.-O. Hahn, G. Kramer, and C. Scully, “Accuracy Assessment Methods for Physiological Model Selection toward Evaluation of Closed-Loop Controlled Medical Devices,” *PLoS One*, vol. 16, no. 4, p. e0251001, 2021, doi: 10.1371/journal.pone.0251001.